

Molecular Energies and Properties from Density Functional Theory: Exploring Basis Set Dependence of Kohn–Sham Equation Using Several Density Functionals

ANDREW C. SCHEINER,* JON BAKER,[†] and JAN W. ANDZELM

Molecular Simulations, Inc., 9685 Scranton Road, San Diego, California 92121-3752

Received 5 April 1996; accepted 8 August 1996

ABSTRACT

The performance of four commonly used density functionals (VWN, BLYP, BP91, and Becke's original three-parameter approximation to the adiabatic connection formula, referred to herein as the adiabatic connection method or ACM) was studied with a series of six Gaussian-type atomic basis sets [DZP, 6–31G**, DZVP, TZVP, TZ2P, and uncontracted aug-cc-pVTZ (UCC)]. The geometries and dipole moments of over 100 first-row and second-row molecules and reaction energies of over 300 chemical reactions involving such molecules were computed using each of the four density functionals in combination with each of the six basis sets. The results were compared to experimentally determined values. Based on overall mean absolute theory versus experiment errors, it was found that ACM is the best choice for predictions of both energies of reaction [overall mean absolute theory versus experiment error (MATvEE) of 4.7 kcal/mol with our most complete (UCC) basis set] and molecular geometries (overall MATvEE of 0.92 pm for bond distances and 0.88° for bond angles with the UCC basis set). For routine calculations with moderate basis sets (those of double- ζ type: DZP, 6–31G**, and DZVP) the DZVP basis set was, on average, the best choice. There were, however, examples of reactions where significantly larger basis sets were required to achieve reasonable accuracy (errors ≤ 5 kcal/mol). For dipole moments, ACM, BP91, and BLYP performed comparably (overall MATvEE of 0.071, 0.067, and 0.059 debye, respectively, with the UCC

*Author to whom all correspondence should be addressed.

E-mail: scheiner@msi.com

[†]Present address: Department of Chemistry, University of Arkansas, Fayetteville, AR 72701.

basis set). Basis sets that include additional polarization functions and diffuse functions were found to be important for accurate density functional theory predictions of dipole moments. © 1997 by John Wiley & Sons, Inc.

Introduction

In recent years, the application of methods based on density functional theory (DFT) to problems in molecular quantum chemistry has grown enormously due to the favorable accuracy and CPU cost of DFT methods^{1–5} and the development and distribution of high quality DFT-based quantum chemistry software packages.^{6–9}

While the computational approach taken by the developers of the various DFT codes may differ, the basic equation being solved, the Kohn–Sham equation, is common throughout.¹⁰ In its simplest form the Kohn–Sham equation can be written as a pseudoeigenvalue equation of the form

$$\mathbf{F}\phi_i = \varepsilon_i\phi_i, \quad (1)$$

where the Kohn–Sham matrix operator, \mathbf{F} , is a sum of the electron kinetic energy term, the electron–nucleus and electron–electron Coulomb potential terms, and the DFT exchange–correlation potential term,

$$\mathbf{F} = -\frac{1}{2}\nabla^2 + V_{\text{Coulomb}} + \mu^{xc}. \quad (2)$$

In eq. (1) the eigenvectors $\{\phi_i\}$ and eigenvalues $\{\varepsilon_i\}$ correspond to molecular orbitals and their energies.

The critical feature of Kohn–Sham DFT is the exchange–correlation potential, $\mu^{xc}[\rho(\mathbf{r})]$ (where $\rho(\mathbf{r})$ is the exact electron density), that by definition is the idealized one-electron potential that exactly accounts for all of the electron–electron interactions that cannot be accounted for by the classical Coulomb potential. The exchange–correlation energy associated with this potential is given by

$$E^{xc} = \int U^{xc}[\rho(\mathbf{r})] d\mathbf{r}, \quad (3)$$

where $U^{xc}[\rho(\mathbf{r})]$ is the idealized, exact density functional. The exchange–correlation potential can be formally expressed as the functional derivative

of the exchange–correlation energy.¹¹

$$\mu^{xc} = \frac{\delta E^{xc}[\rho(\mathbf{r})]}{\delta \rho(\mathbf{r})} = \frac{\partial U^{xc}}{\partial \rho} - \frac{d}{d\mathbf{r}} \cdot \frac{\partial U^{xc}}{\partial \nabla \rho} + \cdots + (-1)^n \left(\frac{d^n}{d\mathbf{r}^n} \cdot \frac{\partial U^{xc}}{\partial \nabla^n \rho} \right). \quad (4)$$

One should note the similarity between the Kohn–Sham equation [eqs. (1) and (2)] and the Hartree–Fock (HF) equation in which μ^{xc} , the exchange–correlation potential of eq. (2), is replaced by the exact HF exchange operator. However, unlike the HF approach (for which the exact solution of the pseudoeigenvalue equation yields a result that excludes electron correlation explicitly, and is therefore, in general, wrong), solution of the Kohn–Sham equation can, in principal, give the exact ground state electron density and, thus, exact ground state molecular properties within the Born–Oppenheimer approximation.

In current practical applications of Kohn–Sham DFT in molecular quantum chemistry, however, one must make two significant approximations. First, a real, closed functional form for the exchange–correlation density functional, U^{xc} , must be chosen that is designed to approximate the idealized, exact (yet unknown) density functional. Second, the molecular orbitals must be constructed from a finite set of basis functions (as is done in most molecular applications of HF theory and in traditional post-HF methods as well).

Regarding the choice of an exchange–correlation functional, the design of increasingly accurate functionals is now, and will continue to be for the foreseeable future, an area of active research. Although it can be viewed as a single functional that incorporates the effects of both exchange and correlation, in all of the functionals developed and in practical use today the two components, exchange and correlation, are separable and are often developed independently.

The earliest density functionals, such as Slater's X_α method,¹² were exchange only and were mainly used in extended systems. One of the first functionals to include electron correlation was developed by Vosko, Wilk, and Nusair (VWN)¹³ by

parameterizing the exact uniform gas results of Ceperley and Alder.¹⁴ This is an example of a so-called *local* functional, because it is a functional of the density only. Most of the functionals popular today for molecular calculations involve not only the density but also its (first) derivative. This was introduced in order to better describe regions where the density changes rapidly. Such functionals, termed *nonlocal* (or *gradient corrected*), include Becke's 1988 exchange functional (B88),¹⁵ Lee, Yang, and Parr's correlation functional (LYP),¹⁶ and Perdew and Wang's 1991 correlation functional (PW91).¹⁷

In addition to these "pure" DFT exchange-correlation functionals, recent work by Becke¹⁸ suggests that mixing a portion of the exact HF exchange in with the DFT exchange correlation is necessary for further improvements in accuracy. Such "hybrid" HF-DFT functionals are increasing in popularity; there are currently several variants in the literature, and they do indeed give significantly better results on average than do the pure functionals, both local and nonlocal.^{19–31} Recently these hybrid methods were used to improve upon very accurate schemes for calculating reaction energies.^{32,33}

As noted above, the limitation of a finite basis set is not unique to DFT, and, based partly on experience with traditional HF based methods, a variety of basis set types were employed in molecular DFT calculations. These included Gaussian-type atom-centered functions, Slater-type atom-centered functions, numerical atom-centered functions, and, less frequently, plane waves and augmented plane waves, which are more suitable for extended periodic systems.

The molecular orbitals [MO; ϕ_i in eq. (1)] are constructed as linear expansions of the basis functions $\{\chi_\mu\}$

$$\phi_i(\mathbf{r}) = \sum_{\mu} C_{i\mu} \chi_{\mu}(\mathbf{r}), \quad (5)$$

where the $C_{i\mu}$ linear expansion coefficients are variationally optimized subject to the constraint of MO orthonormality,

$$\int \phi_i^*(\mathbf{r}) \phi_j(\mathbf{r}) d\mathbf{r} = \delta_{ij}. \quad (6)$$

While each of these types of basis sets has their advantages and disadvantages, the most recent developments in molecular DFT focused on atom-

centered Gaussian-type functions because they allow the theory and computer code to be cast in direct analogy with that of standard HF. This takes advantage of the sophisticated features and functionality of mature HF based software.⁴ Furthermore, because of the very promising results reported recently using hybrid functionals,^{19–31} there is clearly a need for calculation of the exact HF exchange within the realm of DFT.

For the reasons stated above, in the present study we approached the Kohn–Sham problem in analogy to traditional HF and attempted to evaluate and quantify the errors in molecular properties predicted by such a methodology. In so doing, we used several of the popular DFT functionals including Becke's original three-parameter approximation to the "adiabatic connection" formula¹⁸ (herein referred to as the adiabatic connection method or ACM), in combination with a variety of atom-centered Gaussian-type basis sets. The Gaussian basis sets employed include moderate-sized basis sets developed for, and in long-time use in, HF calculations, moderate-sized basis sets derived from HF basis sets but optimized for (local) DFT atoms; and, in an attempt to approach basis set saturation (in *s*, *p*, *d*, and *f* basis functions) for the various functionals, large, uncontracted basis sets developed for explicitly correlated atoms (singles + doubles configuration interaction out of an HF reference determinant).

In this study we address several important questions related to basis set and functional choice in practical molecular applications of DFT: Which of the currently available, moderate-sized basis sets is the best choice to use in conjunction with each of the density functionals? Which DFT functional gives the best predictions for molecular energies—dipole moments? equilibrium molecular geometries? How do the various functionals perform as we approach basis set saturation (seemingly a good measure of the correctness of each of the density functionals)?

We investigated the equilibrium geometries and dipole moments of 108 small- to medium-sized molecules and the energetics of 305 reactions involving these molecules. Included were atomization energies, bond-dissociation energies, heats of hydrogenation and oxygenation, and isomerization energies. These results were compared to experimental measurements in order to evaluate the performance of the density functionals and the basis sets.

In the following we present the details of our Kohn–Sham DFT methodology and the computations performed in the present study; a comparison of our computational results to known experimental values, and a discussion and analysis of our results with regard to the quality of the functionals and basis sets.

Computational Procedure

DFT METHODOLOGY

As discussed in the Introduction, the self-consistent Kohn–Sham procedure can be formulated in such a way that it resembles standard HF theory with a Fock matrix given by

$$\mathbf{F} = \mathbf{H} + \mathbf{J} + \mathbf{K}^{xc}. \quad (7)$$

In common with several other authors, notably the Johnson⁴ and Handy⁵ groups, we adopted a Gaussian-based approach in which the one-electron (\mathbf{H}) and two-electron (\mathbf{J}) Coulomb matrices were evaluated in essentially exactly the same way as in standard HF theory, with the elements of the DFT exchange-correlation matrix, which formally replaces the usual exchange-only \mathbf{K} matrix in HF theory, evaluated by numerical integration over a series of atom-centered grids.

We implemented our self-consistent Kohn–Sham procedure within the *ab initio* program *Turbomole*,³⁴ originally developed by Ahlrichs and coworkers.³⁵ Specifically, we modified the self-consistent field (SCF) energy and analytic first and second derivative modules of *Turbomole* such that we had the flexibility to construct the elements of the Fock/Kohn–Sham matrix as

$$F_{\lambda\sigma} = H_{\lambda\sigma} + \sum_{\kappa\delta} P_{\kappa\delta} (\lambda\sigma | \kappa\delta) + K_{\lambda\sigma}, \quad (8)$$

where $H_{\lambda\sigma}$ are elements of the one-electron Hamiltonian matrix, $P_{\kappa\delta}$ are elements of the density matrix, and $(\lambda\sigma | \kappa\delta)$ are the usual four-index, two-electron atomic orbital (AO) integrals,

$$(\lambda\sigma | \kappa\delta) = \int d\mathbf{r}_1 d\mathbf{r}_2 \chi_\lambda^*(\mathbf{r}_1) \chi_\sigma(\mathbf{r}_1) \times (|\mathbf{r}_1 - \mathbf{r}_2|)^{-1} \chi_\kappa^*(\mathbf{r}_2) \chi_\delta(\mathbf{r}_2).$$

Note that while we did not specify any particular spin characteristics for the quantities in eq. (8), we applied this formalism to both closed-shell and unrestricted open-shell type Fock/Kohn–Sham

equations. $K_{\lambda\sigma}$ may be evaluated using either

1. exact HF exchange,
2. Slater exchange ($\rho^{4/3}$)¹²,
3. Becke's gradient correction to exchange (B88),¹⁵
4. Vosko et al., parameterization of the exact uniform gas results of Ceperley and Alder (VWN local correlation)^{13,14}
5. Lee and colleagues gradient correction to correlation (LYP),¹⁶
6. Perdew and Wang's gradient correction to correlation (PW91),¹⁷
7. any combination of any number of the above (including weighted combinations such as Becke's ACM¹⁸).

The HF exchange is calculated in the standard way

$$K_{\lambda\sigma}^{\text{exact}} = -\frac{1}{2} \sum_{\kappa\delta} P_{\kappa\delta} (\lambda\kappa | \delta\sigma), \quad (9)$$

using the same two-electron integrals that are used to construct the Coulomb term.

The DFT contributions to $K_{\lambda\sigma}$ can be formally expressed as

$$K_{\lambda\sigma}^{xc} = (\lambda | \mu^{xc} | \sigma) = \int \chi_\lambda^*(\mathbf{r}) \chi_\sigma(\mathbf{r}) \mu^{xc}[\rho(\mathbf{r})] d\mathbf{r}. \quad (10)$$

The standard technique for evaluating multicenter molecular integrals, such as that found in eq. (10), is to partition them into single-center atomic integrals that are then evaluated numerically on atomic grids. Thus,

$$K_{\lambda\sigma}^{xc} = \sum_A \sum_i w_{Ai} \mu^{xc}[\rho(\mathbf{r}_{Ai})] \chi_\lambda^*(\mathbf{r}_{Ai}) \chi_\sigma(\mathbf{r}_{Ai}), \quad (11)$$

where the first summation runs over all the atoms in the system and the second is over the numerical quadrature grid points associated with that atom. The w_{Ai} are quadrature weights, and $\mathbf{r}_{Ai} = \mathbf{R}_A + \mathbf{r}_i$, where \mathbf{R}_A is the position vector of atom A , and \mathbf{r}_i is the vector from atom A to grid point i of a spherical grid centered on A .

The single-center integrals in eq. (11) are separated into radial and angular parts, with spherical surfaces defined at each point on a radial grid on which to carry out the angular integrations. This corresponds to quadrature on the surface of a sphere, and there are several formulae available to do these integrations. The most popular at the

present time are probably those due to Lebedev.³⁶ The majority of DFT grid designs and quadrature schemes in use today stem from the work of Becke³⁷ and Delley,³⁸ especially as regards selection of the partition function and quadrature weights.

Originally, we based our grid on the scheme used in *DMol*, which was developed by Delley.³⁸ Recently, a high quality grid that uses a modification of the Becke scheme with improved radial integration was developed by Treutler and Ahlrichs.³⁹ This grid, which offers increased accuracy over previous integration schemes as well as fully exploiting almost all standard point group symmetry up to and including I_h , was designed and implemented within *Turbomole*; consequently, we have now adopted the Treutler–Ahlrichs grid as our standard. (We used grid 3 as defined in ref. 39 as our default grid; ignoring symmetry this typically results in approximately 3300 points for hydrogen, 5900 points for first-row atoms, and 6600 points for second-row atoms.)

We illustrate our DFT implementation within *Turbomole* by taking as an example the construction of the exchange–correlation matrix, \mathbf{K}^{xc} . This is shown schematically below.

For each unique grid point, \mathbf{r}_{Ai}

1. construct AOs $\chi_\sigma(\mathbf{r}_{Ai})$ and, if necessary, AO derivatives $\chi'_\sigma(\mathbf{r}_{Ai})$ $\{\sigma = 1, \text{ number of basis functions, NBF}\}$
2. construct an indexing array indicating which AOs have magnitude (at \mathbf{r}_{Ai}) greater than threshold (see below for definition of threshold);
3. from occupied MO coefficients and $\chi_\sigma(\mathbf{r}_{Ai})$, form $\rho(\mathbf{r}_{Ai})$; note that this step is vectorizable of order $\text{NOcc} \times \text{NBF}$ (where NOcc is the number of occupied orbitals);
4. save $\rho(\mathbf{r}_{Ai})$ in core memory;
5. form difference density using density from current and previous SCF iterations;
6. if both current and difference density at \mathbf{r}_{Ai} have magnitude greater than threshold, then
 - i. calculate exchange–correlation potential, $\mu^{xc}(\mathbf{r}_{Ai})$, and, if necessary, $(\mu^{xc})'(\mathbf{r}_{Ai})$;
 - ii. save $\mu^{xc}(\mathbf{r}_{Ai})$ and its contribution to exchange–correlation energy ($E^{xc}(\mathbf{r}_{Ai})$ in core memory;
 - iii. form a difference potential using $\mu^{xc}(\mathbf{r}_{Ai})$ from current and previous SCF iterations;

- iv. if the difference potential has a magnitude greater than threshold, then calculate the contribution to the difference exchange–correlation matrix (\mathbf{K}^{xc}) at \mathbf{r}_{Ai} by carrying out numerical integration using the difference potential and AO vector; note that this step is vectorizable of order $\text{NBF} \times \text{NBF}$.

There are two features of our implementation to which we draw specific attention. The first is that the *outer* loop is over (symmetry-unique) grid points, which is different from most other implementations (e.g., in *DMol* blocks of grid points form the *inner* loop; a similar situation holds for the DFT implementations in both *Gaussian 92/94*⁴⁰ and *CADPAC*⁴¹). The only other implementation we are aware of that is similar to ours in general outline is that of van Wüllen,⁴² which was also developed using *Turbomole* but was derived quite independently.

The second feature is that we construct *difference* quantities, and ultimately, a difference \mathbf{K}^{xc} matrix. This enables us to more easily adapt our code to the standard direct SCF algorithm within *Turbomole* that, in common with most other direct SCF codes, uses difference densities when constructing the Fock matrix.

There are three places in the code where sparsity is directly utilized. The first is in filtering out those basis functions whose values at the current grid point are considered too small to contribute; this has a major impact on the time taken both to construct the density at that grid point and to do the final numerical integration once the potential has been determined. Furthermore, once the density has been calculated, if either it or the density difference from the previous cycle is below the density cutoff, then no further action is taken (i.e., potential evaluation and numerical integration are avoided for the current grid point, and we move to a new grid point). Finally, there is a chance to avoid doing the numerical integration after the potential at the grid point has been found; if the difference potential is below the cutoff the current point is rejected.

These three cutoff thresholds [steps 2, 6, and 6(iv) in the above schematic] do not have the same value on every cycle; they are gradually reduced as convergence is attained. The formula we use is:

$$\begin{aligned} \text{thrsh} &= \text{MIN}(\text{thrmax}, \text{ddnrm} \times \text{thrmax}) \\ \text{thrsh} &= \text{MAX}(\text{thrsh}, \text{thrmin}), \end{aligned} \quad \text{and then}$$

where $\text{thrmax} = 10^{-8}$, $\text{thrmin} = 10^{-16}$, and ddnm is the norm of the difference density matrix (a measure of the SCF convergence). The various thresholds thus take values between 10^{-8} at the start of the SCF procedure to 10^{-16} at the end. Note that on the first cycle, because the quality of the density (i.e., the starting MOs) is not known, all thresholds are set to thrmin .

The most time consuming steps in our computation of \mathbf{K}^{xc} are construction of the density (NPoint*NOcc*NBF, where Npoint is the total number of grid points, NOcc is the number of occupied MOs, and NBF is as previously) and the final numerical integration (NPoint*NBF*NBF). Both steps are thus formally $O(N^3)$, with N being roughly a measure of the size of the system. However, as indicated in the algorithm schematic above, both steps are vectorizable and both can fully utilize sparsity, making them in practice $O(N^{1.5})$ or less. Thus, the bottleneck in this approach is the time taken to calculate and treat the Coulomb integrals that, although formally $O(N^4)$, is in practice, with due consideration of sparsity, approximately $O(N^{2.5})$. For large systems then, the cost of the DFT component (the calculation of \mathbf{K}^{xc}) becomes insignificant and DFT computations are essentially the same cost as a standard HF calculation, a fact clearly pointed out by Johnson et al.⁴

Although we illustrated our DFT implementation by considering the SCF energy, the same general code structure carries over straightforwardly to calculation of the DFT component of the gradient as well. Here we do not need to construct any difference quantities because calculation of the derivative quantities is not iterative (we use a threshold of 10^{-12} for the density and potential cutoffs). The same comments as regards timing with increasing system size that were made for the SCF energy also hold, even more so, for the gradient.

Finally, we comment briefly on the use of quadrature weight derivatives in the calculation of the DFT energy gradient. The multicenter exchange-correlation integral, eq. (3), can be partitioned in terms of single-center integrals in exactly the same way as was done for the \mathbf{K}^{xc} matrix elements [eqs. (10) and (11)] to yield

$$E^{xc} = \sum_A \sum_i w_{Ai} U^{xc}[\rho(\mathbf{r}_{Ai})]. \quad (12)$$

Formally differentiating this with respect to nu-

clear displacement gives^{4, 43}

$$\nabla_B E^{xc} = \sum_A \sum_i [w_{Ai} \nabla_B U^{xc} + \nabla_B w_{Ai} U^{xc}]. \quad (13)$$

Thus, there are two terms in the energy derivative: one involving the derivative of the density functional and the second involving the derivative of the quadrature weights. The latter term is often ignored and indeed should tend to zero with a sufficiently large number of grid points (however, this needs to be a very large number). Although leaving out the quadrature weight term often results in a noticeable loss of translational invariance (of order 10^{-4}) in the Cartesian gradient vector, we demonstrated elsewhere⁴⁴ that, for the good quality grids used in this work, this is essentially cosmetic and final optimized structures and energetics are the same to chemical accuracy whether quadrature weight derivatives are included in the gradient or not. Consequently for the most part, we omitted this term when calculating our DFT gradients.

MOLECULAR APPLICATIONS

We applied our DFT methodology to predict the equilibrium geometries, energies, and dipole moments of 108 small molecules comprising H, Li, B—F, Na, Si—Cl, as well as the total atomic energies of each such atom in its ground electronic state. The full set of molecules examined in the present study is shown in Figure 1. The set includes 54 of the 55 molecules considered by Pople and coworkers in their well-known G1⁴⁵ and G2⁴⁶ studies, plus an additional 54 relatively larger molecules including seven cyclic systems and several molecules that proved difficult for standard *ab initio* methods, such as FOOF. We also included various isomer sets, e.g., three isomers of C_3H_4 and four of CH_2N_2 .

For each of the atoms and molecules, calculations were performed using four density functionals combined with six Gaussian basis set (i.e., a total of 24 sets of DFT calculations/atom/molecule).

The four functionals employed are:

1. VWN (local Slater exchange + local VWN correlation),
2. BP91 (B88 gradient corrected exchange + PW91 gradient corrected correlation),
3. BLYP (B88 gradient corrected exchange + LYP gradient corrected correlation), and

H ₂	lithium hydride (LiH)	difluoroborane (BF ₂ H)	BH ₂
BN	BO	BS	diborane (B ₂ H ₆)
CH	CH ₂ (¹ A ₁)	CH ₂ (³ B ₁)	methyl radical (CH ₃)
methane (CH ₄)	NH	NH ₂	ammonia (NH ₃)
hydroxyl radical (OH)	water (H ₂ O)	hydrogen fluoride (HF)	Li ₂
lithium fluoride (LiF)	acetylene (HCCH)	vinylidene (CCH ₂)	ethylene (H ₂ CCH ₂)
ethane (H ₃ CCH ₃)	propyne (H ₃ CCCH)	allene (H ₂ CCCH ₂)	cyclopropene (CHCH ₂ CH)
propene (H ₃ CCHCH ₂)	cyclopropane (CH ₂ CH ₂ CH ₂)	CN	hydrogen cyanide (HCN)
hydrogen isocyanide (HNC)	HCNO	HNCO	HCP
carbon monoxide (CO)	formyl radical (HCO)	HPO	HNO
HNO ₃	formaldehyde (H ₂ CO)	HCOH	formic acid (HCOOH)
methyl amine (CH ₃ NH ₂)	methyl phosphine (CH ₃ PH ₂)	methanol (CH ₃ OH)	acetaldehyde (CH ₃ CHO)
vinyl alcohol (CH ₂ CHOH)	ethylene oxide (CH ₂ OCH ₂)	dimethyl ether (CH ₃ OCH ₃)	N ₂
cis-diimine (HNNH)	trans-diimine (HNNH)	hydrazine (H ₂ NNH ₂)	NH ₂ CN
HNCNH	diazomethane (CH ₂ N ₂)	diazirine (NCH ₂ N)	O ₂
hydrogen peroxide (HOOH)	F ₂	FCN	perfluoromethane (F ₂ CO)
perfluoroperoxide (FOOF)	FOH	NF	NSF
carbon dioxide (CO ₂)	SiH	SiH ₂ (¹ A ₁)	SiH ₂ (³ B ₁)
SiH ₃	SiH ₄	PH ₂	PH ₃
SH	hydrogen sulfide (H ₂ S)	hydrogen chloride (HCl)	Na ₂
Si ₂	P ₂	S ₂	Cl ₂
sodium chloride (NaCl)	SiO	CS	SO
ClO	ClO ₂	Cl ₂ O	cyclopropanone (CH ₂ COCH ₂)
chloromethane (CH ₃ Cl)	methanethiol (CH ₃ SH)	difluoromethane (CH ₂ F ₂)	CH ₂ NH
disilaethane (H ₃ SiSiH ₃)	fluoromethane (CH ₃ F)	NOF	SO ₂
SO ₃	NO ₂	1,2,5-oxadiazole (CHNONCH)	1,3,4-oxadiazole (NCHOCHN)
PO	HOCl	NOCI	ClF

FIGURE 1. List of molecules included in the present study.

- the adiabatic connection method (ACM) as defined in ref. 18.

These functionals were chosen because they represent the currently most popular functionals for applications to molecular systems.

The six basis sets selected for the present study consist of

- DZP: the HF atom-optimized, double- ζ basis sets of Schäfer et al.⁴⁷ + a single polarization set;
- 6-31G**: the standard HF atom-optimized valence double- ζ basis set⁴⁸ + a single polarization set;
- DZVP: the local DFT atom-optimized, valence double- ζ basis sets of Godbout et al.⁴⁹ + a single polarization set;
- TZVP: the local DFT atom-optimized, valence triple- ζ basis sets of Godbout et al.⁴⁹ + a single polarization set;

- TZ2P: the HF atom-optimized, triple- ζ basis set of Schäfer and coworkers⁴⁷ + two polarization sets; and

- uncontracted aug-cc-pVTZ (UCC): the augmented correlation consistent valence triple- ζ basis sets of Dunning et al.⁵⁰ In the present study, we used these basis sets entirely *uncontracted* in order to approach basis set saturation in the *s*, *p*, *d*, *f* space. Thus, we have H(7s3p2d), B—F(11s6p3d2f), and Si—Cl(16s10p3d2f).

The first five basis sets were chosen because they represent a selection of moderate-size Gaussian basis sets currently popular for practical applications of *ab initio* electronic structure methods. Although the UCC basis set is not appropriate for routine applications (because it would become impractically large for most molecules), it was chosen for two reasons. First, it represents our attempt to approach basis set saturation (in *s*, *p*, *d*, and *f* functions) of the four functionals. The UCC results

were used as a reference against which to compare the performance of the moderate-size basis sets and, as noted above, to indicate the “correctness” of each of the four functionals as one approaches basis set saturation. Second, of the various large basis sets that we could have chosen to serve as a reference, we chose the correlation consistent type of basis for this purpose because it was designed (albeit in a contracted form) from CISD calculations (which include electron correlation) and should be a reasonable choice for DFT calculations that also include electron correlation.

For all basis sets, pure *d* and *f* function sets (i.e., the 5*d* and 7*f* representations) were used.

In addition to the DFT calculations, we also carried out HF and second-order Møller–Plesset (MP2) calculations with the 6–31G** basis set in order to compare results using these two traditional *ab initio* methods to those from the various density functionals.

Results and Discussion

Because the amount of raw data that was generated during the course of the present study was quite large (approximately 2500 atomic/molecular energies and dipole moments, 8000 heats of reaction, and 8500 geometrical parameters), we have not included it herein. Rather, we present statistical analyses of our data. Obviously, with such a large amount of data, we could not practically consider every aspect of the computed molecular energies and properties. However, we certainly anticipate that other researchers may wish to use our data to explore specific details that we did not address. Therefore, we have made this data available as Supplementary Material.⁵¹

HEATS OF REACTION

From the energies of the 108 molecules considered (at their optimized geometries) and their constituent atoms, the heats of 305 chemical reactions were examined. The reactions, listed individually as part of our Supplementary Material,⁵¹ were classified as follows:

- 108 atomization reactions (dissociation of a molecule into its constituent atoms),
- 66 bond dissociation reactions (dissociation of one bond),
- 73 hydrogenation reactions (addition of H₂),
- 29 oxygenation reactions (addition of O₂),

- 12 isomerization reactions (energy difference between isomers),
- 8 isodesmic reactions (reactions in which the bond types of the reactants and products are conserved), and
- 40 “other” reactions (including fluorination, chlorination, addition of ammonia, addition of water, bond dissociation/creation involving more than one bond, functional group exchange reactions).

The computational results were adjusted for zero-point vibrational energy (using HF 6–31G* vibrational frequencies scaled by 0.8929) and compared to available experimental results (based on experimentally determined gas-phase heats of formation).⁵²

In Tables I and II we present a comparison of the performance of the 26 computational methods where, for the purposes of the present discussion, we define a computational method to be a particular choice of level of theory and basis set (e.g., VWN with the TZ2P basis set) considered in the present study. We used experimentally determined quantities as the standard against which the computed results were to be evaluated, and, as such, tabulated errors with respect to the experimentally determined heats of reaction for each of the 26 computational methods. Table I includes the mean absolute errors, the standard deviations of the mean absolute errors, and the maximum absolute errors for each method applied to all 305 reactions; as such, this represents the overall performance of each of the computational methods for predictions of the reaction energies studied. Additionally, we tabulated the mean absolute errors for each of the computational methods within various classes of reactions, and these are presented in Table II. Note that we consider the *absolute* deviations, and thus deviations of +*r* and –*r* contribute equally in our statistical analysis (i.e., they do not cancel).

Based on the mean errors with respect to the experimentally determined heats of reaction in Table I, the overall performance of the methods (from best to worst) is

$$\text{ACM} > \text{BP91} > \text{BLYP} \gg \text{VWN}.$$

The DFT basis set dependence for the mean absolute errors of the analysis of all reactions warrants several remarks. First, while the overall trend for the non-local DFT methods (those DFT methods which include gradient corrections in the func-

TABLE I.
Comparison of Theoretical and Experimental Reaction Energies for All 305 Reactions
Considered in Present Study.

Method	$\langle x \rangle \pm \sigma^a$	Maximum ^b
HF, 6–31G**	54.82 \pm 59.83	257.17, $\text{HNO}_3 \rightarrow \text{N} + 3\text{O} + \text{H}$
MP2, 6–31G**	11.86 \pm 11.25	63.11, $\text{NSF} \rightarrow \text{S} + \text{N} + \text{F}$
VWN		
DZP	24.64 \pm 25.29	135.31, $\text{HNO}_3 \rightarrow \text{N} + 3\text{O} + \text{H}$
6–31G**	26.28 \pm 27.28	136.18, $\text{HNO}_3 \rightarrow \text{N} + 3\text{O} + \text{H}$
DZVP	23.28 \pm 24.79	125.11, $\text{HNO}_3 \rightarrow \text{N} + 3\text{O} + \text{H}$
TZVP	24.34 \pm 26.00	125.92, $\text{HNO}_3 \rightarrow \text{N} + 3\text{O} + \text{H}$
TZ2P	23.58 \pm 26.52	132.79, $\text{HNO}_3 \rightarrow \text{N} + 3\text{O} + \text{H}$
UCC	25.56 \pm 28.28	137.70, $\text{HNO}_3 \rightarrow \text{N} + 3\text{O} + \text{H}$
BLYP		
DZP	11.33 \pm 12.79	71.79, $\text{S}_2 + 2\text{O}_2 \rightarrow 2\text{SO}_2$
6–31G**	9.95 \pm 12.50	65.76, $\text{propene} + 9/2\text{O}_2 \rightarrow 3\text{CO}_2 + 3\text{H}_2\text{O}$
DZVP	7.73 \pm 8.79	55.42, $\text{S}_2 + 2\text{O}_2 \rightarrow 2\text{SO}_2$
TZVP	7.17 \pm 7.24	48.98, $\text{S}_2 + 2\text{O}_2 \rightarrow 2\text{SO}_2$
TZ2P	7.35 \pm 7.12	35.18, $\text{S}_2 + 2\text{O}_2 \rightarrow 2\text{SO}_2$
UCC	7.09 \pm 6.97	38.82, $\text{S}_2 + 2\text{O}_2 \rightarrow 2\text{SO}_2$
BP91		
DZP	10.41 \pm 12.23	71.19, $\text{cyclopropane} + 3\text{O}_2 \rightarrow 3\text{CO} + 3\text{H}_2\text{O}$
6–31G**	9.35 \pm 11.81	73.57, $\text{cyclopropane} + 3\text{O}_2 \rightarrow 3\text{CO} + 3\text{H}_2\text{O}$
DZVP	6.91 \pm 8.44	53.35, $\text{cyclopropane} + 3\text{O}_2 \rightarrow 3\text{CO} + 3\text{H}_2\text{O}$
TZVP	6.43 \pm 7.54	48.48, $\text{S}_2 + 2\text{O}_2 \rightarrow \text{SO}_2$
TZ2P	6.69 \pm 7.37	42.04, $\text{cyclopropane} + 3\text{O}_2 \rightarrow 3\text{CO} + 3\text{H}_2$
UCC	6.50 \pm 7.58	41.21, $\text{cyclopropane} + 3\text{O}_2 \rightarrow 3\text{CO} + 3\text{H}_2\text{O}$
ACM		
DZP	9.48 \pm 10.70	77.61, $\text{S}_2 + 2\text{O}_2 \rightarrow 2\text{SO}_2$
6–31G**	8.05 \pm 10.00	65.22, $\text{S}_2 + 2\text{O}_2 \rightarrow 2\text{SO}_2$
DZVP	7.37 \pm 8.29	59.21, $\text{S}_2 + 2\text{O}_2 \rightarrow 2\text{SO}_2$
TZVP	6.51 \pm 7.59	54.27, $\text{S}_2 + 2\text{O}_2 \rightarrow 2\text{SO}_2$
TZ2P	5.64 \pm 5.88	38.31, $\text{S}_2 + 2\text{O}_2 \rightarrow 2\text{SO}_2$
UCC	4.74 \pm 6.21	43.10, $\text{S}_2 + 2\text{O}_2 \rightarrow 2\text{SO}_2$

Tabulated quantities are mean absolute theory vs. experiment errors of heats of reaction (kcal/mol) \pm standard deviation of the mean absolute error (kcal/mol) and maximum absolute error (kcal/mol) (with reaction for which maximum error occurs also indicated).

A list of reactions considered in the present study may be obtained as Supplementary Material; see ref. 51.

^aMean absolute deviation from experiment \pm standard deviation of the mean for all 305 reactions.

^bMaximum absolute deviation from experiment followed by the reaction for which the maximum deviation occurs.

tional—BLYP, BP91, and ACM) is as one would expect for methods that include treatment of electron correlation (i.e., the mean absolute errors generally decrease as the basis set approaches saturation), this is not so for the VWN functional. In the case of VWN, the mean error remains between 23 and 27 kcal/mol for all basis sets employed; and, in fact, the mean error for the largest (UCC) basis set is exceeded only by that for the 6–31G** basis set. Clearly, large errors in calculation of molecular energies not attributable to basis set deficiencies are present in the VWN functional (and, presumably, other such local density functionals). Consequently, such local functionals should generally

not be used to model chemical reaction energetics. There is one notable exception to this general rule: oxygenation reactions (see column 5 of Table II and the discussion of oxygenation reactions, below).

The second point to note regarding overall basis set dependence for the analysis including all reactions, is that, of the moderate-size, double- ζ type basis sets (DZP, 6–31G**, and DZVP), the DZVP basis set, which was optimized for local DFT atoms, is superior. For the NLDFT functionals, the DZVP basis set is, on average, 1–3 kcal/mol better than 6–31G** and 2–4 kcal/mol better than DZP. In the case of VWN, DZVP is also better, on average,

TABLE II. **Mean Absolute Theory Vs. Experiment Errors of Heats of Reaction (kcal / mol) for Individual Reaction Classes.**

Method	Reactions						
	Atom ^a	BD ^b	H ₂ ^c	O ₂ ^d	IsoM ^e	IsoD ^f	Other ^g
HF, 6–31G**	119.23	58.85	8.46	44.52	6.88	2.51	4.32
MP2, 6–31G**	22.00	8.79	6.96	11.19	5.13	2.97	4.40
VWN							
DZP	47.01	20.32	11.78	21.86	5.31	7.38	10.28
6–31G**	52.24	22.08	11.29	21.82	5.10	7.50	9.89
DZVP	47.62	19.81	10.36	14.99	5.37	5.03	7.13
TZVP	52.07	22.17	9.62	13.16	5.59	4.88	6.12
TZ2P	50.77	21.52	8.27	11.58	5.16	5.01	5.75
UCC	56.41	23.65	8.54	11.70	5.53	4.66	5.65
BLYP							
DZP	10.16	5.78	13.49	28.61	4.54	4.53	9.75
6–31G**	6.97	5.50	13.15	29.14	3.91	4.37	8.29
DZVP	7.36	5.01	7.27	21.50	4.16	3.42	5.90
TZVP	6.86	4.80	7.40	16.42	4.81	3.20	5.77
TZ2P	7.44	4.89	7.83	15.41	4.54	3.21	5.91
UCC	7.07	5.20	7.26	15.00	4.49	2.90	5.43
BP91							
DZP	9.71	6.27	10.66	27.59	3.99	4.90	8.48
6–31G**	7.39	5.92	10.13	27.62	3.97	4.92	7.64
DZVP	6.44	5.29	5.58	20.71	3.85	3.81	4.88
TZVP	6.20	4.99	5.50	17.25	4.00	3.62	4.33
TZ2P	7.31	5.45	5.49	15.93	3.57	3.68	4.33
UCC	7.03	5.36	5.26	15.94	3.89	3.28	3.81
ACM							
DZP	10.12	6.42	7.92	26.06	3.62	4.34	6.49
6–31G**	6.79	5.65	6.97	26.16	3.89	4.35	6.11
DZVP	8.78	6.41	5.15	18.84	4.04	3.33	3.26
TZVP	7.83	5.93	4.58	15.64	4.25	3.21	2.63
TZ2P	6.51	5.13	3.86	14.35	3.76	3.28	2.61
UCC	4.13	4.44	3.71	14.64	4.09	2.98	2.21

A list of reactions considered in the present study may be obtained as Supplementary Material; see ref. 51.

^aMean absolute deviation from experiment for 108 atomization reactions.

^bMean absolute deviation from experiment for 66 bond dissociation reactions.

^cMean absolute deviation from experiment for 73 hydrogenation reactions.

^dMean absolute deviation from experiment for 29 oxygenation reactions.

^eMean absolute deviation from experiment for 12 isomerization reactions.

^fMean absolute deviation from experiment for 8 isodesmic reactions.

^gMean absolute deviation from experiment for 40 other (see text) reactions.

than either DZP or 6–31G**, although, as noted above, none of the VWN results are satisfactory.

A further distinction can be made between the two pure NLDFT methods (BLYP, BP91) and ACM as regards basis set dependence. In the case of BP91 and BLYP, the performance of these two methods does not change significantly among the four basis sets DZVP, TZVP, TZ2P, and UCC. However, for the ACM method, there is significant improvement in increasing the basis set size from DZVP to TZVP to TZ2P to UCC. Thus, it appears that as one approaches the basis set limits of these three functionals, the adiabatic connection method

is, on average, closer to the exact density functional for molecules involving first- and second-row atoms. It also suggests there may be value in deriving new Gaussian-type basis sets of double- ζ and triple- ζ quality with orbital exponents and contraction coefficients optimized specifically for the ACM functional in that such ACM-specific moderate-size basis sets may provide results closer to the UCC result than do the currently available analogous HF basis sets (DZP, 6–31G**, TZ2P used here) or local DFT basis sets (DZVP and TZVP). Furthermore, there may be value in deriving different sets of ACM coefficients specifically

optimized for particular basis sets in order to improve the performance of ACM when using moderate-size basis sets.

Overall, the quantitative performance of the DFT methods is as follows: For VWN, as noted above, there is little basis set dependence and the mean errors fall in the range of 23–27 kcal/mol. For BLYP, with the best double- ζ type basis set (DZVP) the mean error is 8.1 kcal/mol and improves slightly to 7.3 kcal/mol with the UCC basis set. For BP91, the basis set dependence is similar to that of BLYP; however, on average, the BP91 functional performs better (mean error: DZVP 7.1 kcal/mol, UCC 6.6 kcal/mol). For ACM, with the DZVP basis set the mean error is 7.4 kcal/mol (not quite as good as BP91), but there is continued improvement with the larger basis sets; and with the largest basis set (UCC) the mean error is reduced to 4.9 kcal/mol (no other functional considered in the present study had an overall mean error below 6.5 kcal/mol regardless of basis set choice).

The variance of the results for each of the methods when all reactions are considered is included in the second column of Table I. From a practical standpoint, these quantities are important because they are a measure of how widely the results for each of the methods vary over all reactions (and thus give an indication of the level of confidence one has in using each such method for a reaction for which neither experimental data nor benchmark calculations is available to calibrate the result). The standard deviations of the mean absolute theory versus experiment errors is indicated following the \pm symbol. For five of the six basis sets studied, ACM had the smallest error variance (the exception being the TZVP basis set for which the BLYP variance was slightly less than that for ACM). Overall the ACM/TZ2P method resulted in the smallest variance in the data (a standard deviation of 5.9 kcal/mol). We also note that the difference in variance was quite pronounced between the 6–31G** and DZP results and those of the other four basis sets.

The maximum absolute deviations from the experiment are tabulated in the last column of Table I (along with the chemical reaction for which the maximum deviations occur). For all methods considered, these quantities were quite large (≥ 35 kcal/mol) with the VWN method performing most poorly for the atomization of HNO_3 and the NLDFT methods performing most poorly for oxygenation reactions involving SO_2 (BLYP and ACM) and cyclopropane (BP91). In the case of VWN

these large errors appeared to be mainly due to limitations in the functional (because there is little improvement with the basis set) whereas we did observe a large reduction in the maximum errors for the NLDFT methods with basis set improvements. For particularly difficult reactions such as these, there was still a significant basis set error in the NLDFT methods even with the UCC basis set as seen by further calculations on the atomization of SO_2 (see below and ref. 29). Finally, we note that the method with the smallest maximum absolute deviation was not ACM, but BLYP/TZ2P; and the maximum errors for ACM were, in general, slightly larger than those for either BLYP and BP91.

Considering the mean absolute errors for each reaction class in Table II, qualitatively, the behavior for atomization and bond dissociation reactions was somewhat similar to the overall behavior found in Table I. There were, however, some notable differences. First, for the atomization reactions, the magnitudes of the mean errors for HF, VWN, and MP2 were significantly greater (approximately $2 \times$) than those for all reactions. This observation was, perhaps, not surprising in that, *a priori*, one would certainly consider atomization reactions to be quite challenging for electronic structure methods as one is comparing reactants and products with completely different valence electronic structures. Conversely, the performance of the NLDFT methods for atomization energies was, on average, good (and not greatly different from the performance of these methods overall). Second, in looking closer at the performance of the NLDFT methods one observes that the DFT optimized basis sets (DZVP and TZVP) seemed much better suited to the pure NLDFT methods (BP91 and BLYP) than for the hybrid ACM. As noted above, this suggested that an ACM optimized basis set of double- ζ and triple- ζ types and/or new ACM coefficients specifically tailored for each basis set would be of value. A final point to note is that, for the bond dissociation reaction class, the BLYP method performed consistently better than BP91 (the opposite was found when all reactions were included and for the atomization reactions alone and BLYP performed better than any method with all but the UCC basis set. However, as was the case for the overall performance in Table I, as one approaches the basis set limit of the NLDFT functionals, ACM is superior.

An additional issue with regards to the atomization reactions is to consider how our results compare to other similar studies. Specifically, by

considering only the 54 atomization reactions included in the G1 set of Pople and coworkers,⁴⁵ we can compare our results to the accurate G1 and G2 methods proposed by Pople et al.,^{45,46} Becke's fully numeric⁵³ ACM¹⁸ treatment of these same 54 atomization reactions, and the recent Gaussian basis function work by Bauschlicher and Partridge using an alternative hybrid scheme, B3LYP.^{29,30} B3LYP, first proposed by Stevens et al.,⁵⁴ is based on the same hybrid strategy as the original ACM scheme; however, the LYP correlation functional replaces PW91. In Table III we compare the mean absolute errors with respect to experimental results from the present study with those of Pople et al.,^{45,46} Becke,¹⁸ and Bauschlicher and Partridge.²⁹

First, we note that both the G1 and G2 methods are more accurate (albeit much more expensive) methods for predicting thermochemistry than either of the implementations of the three parameter adiabatic connection method (ACM or B3LYP) tabulated here. Second, regarding basis set dependence, in general, the data in Table III indicate that as the basis set was improved, the results for both hybrid methods were improved. This was not surprising in that we certainly would expect that Becke's numeric ACM values would be the best possible ACM result one could achieve, on average, for this set of 54 atomization energies (because the ACM coefficients were optimized using a fully numeric approach for the G1 set of reactions). In principal, this would not necessarily hold true for B3LYP; but, as indicated by the data in Table III, in practice this does appear to be true for B3LYP as well. One could indeed attempt to improve the ACM or B3LYP results for any basis set by reoptimizing the ACM coefficients for that particular basis set using the 54 atomization reactions or, in general, any set of reactions for which experimental results are well established. For comparison, we also included the BP91 results from the present study along with Becke's numeric BP91 results from 1992.⁵⁵ Unlike ACM, one would not necessarily expect the numeric (basis set limit) BP91 results to give the best possible BP91 heats of reaction for this (or any other) set of reactions. This was borne out by the fact that the DZVP and TZVP basis sets produced the lowest mean absolute deviation from the experiment for this functional.

Based on the comparison in Table III, the UCC basis set appears to be a reasonably good approximation to the basis set limit for this set of reactions (0.7 kcal/mol difference between the UCC and numeric ACM mean absolute errors vs. experi-

TABLE III. Mean and Maximum Absolute Deviations From Experimental Atomization Energies (kcal/mol) for 54 Atomization Reactions Included in G1 Study.⁴⁵

Method	Mean Absolute Error	Maximum Absolute Error
G1 ^a	1.6	7.4(SO ₂)
G2 ^b	1.2	5.1(SO ₂)
B3LYP ^c		
6-31G*	5.1	31.5(SO ₂)
aug-cc-pVTZ	2.5	18.2(SO ₂)
aug-cc-pVTZ + <i>d</i>	2.2	9.7(SO ₂)
6-311 + G(3df, 2p)	2.1	8.4(SO ₂)
ACM		
DZP ^d	6.3	37.2(SO ₂)
6-31G** ^d	4.8	29.4(SO ₂)
DZVP ^d	5.1	33.8(SO ₂)
TZVP ^d	4.4	31.8(SO ₂)
TZ2P ^d	3.1	16.4(SO ₂)
UCC ^d	3.0	14.8(SO ₂)
Numeric ^e	2.3	6.3(SiO)
BP91		
DZP ^d	6.2	35.6(H ₂ O ₂)
6-31G** ^d	5.1	19.6(O ₂)
DZVP ^d	3.7	13.9(SO ₂)
TZVP ^d	3.7	13.2(O ₂)
TZ2P ^d	4.5	16.1(O ₂)
UCC ^d	5.2	19.0(O ₂)
Numeric ^f	5.5	18.4(CO ₂)

^aRef. 45: geometries from MP2/6-31G*; zero point vibrational energies (ZPVE) from scaled HF/6-31G* harmonic vibrational frequencies (at HF/6-31G* geometry).

^bRef. 46: geometries from MP2/6-31G*; ZPVE from scaled HF/6-31G* harmonic vibrational frequencies (at HF/6-31G* geometry).

^cRef. 29: geometries from B3LYP/6-31G*; ZPVE from scaled B3LYP/6-31G*; B3LYP energies determined self-consistently.

^dPresent study: geometries optimized using same method as that used for energies: ZPVE from scaled HF/6-31G* harmonic vibrational frequencies (at HF/6-31G* geometry); ACM energies determined self-consistently.

^eRef. 18: geometries from numeric local DFT; ZPVE from scaled HF/6-31G* harmonic vibrational frequencies (at HF/6-31G* geometry); ACM energies determined perturbatively.

^fRef. 55: geometries from numeric local DFT; ZPVE from scaled HF/6-31G* harmonic vibrational frequencies (at HF/6-31G* geometry); BP91 energies determined perturbatively.

ment and 0.3 kcal/mol difference between the UCC and numeric BP91 quantities). However, such a comparison is, in fact, misleading. When we calculated the mean absolute errors between the ACM/UCC and numeric ACM heats of reaction

(i.e., we compared the 54 ACM/UCC heats of reaction from the present study to the 54 numeric ACM heats of reaction tabulated in ref. 18 and calculated the mean absolute error between these two sets of 54 numbers with no reference to the experiment), this quantity was 2.3 kcal/mol (not 0.7 kcal/mol). Similarly, when we carried out the same analysis for BP91, the difference between our UCC results and the numeric results of Becke was 2.2 kcal/mol (not 0.3 kcal/mol). Thus, basis set deficiencies remained even with the UCC basis set, and such deficiencies tend to be masked by cancellation of errors (basis set errors + errors in the functionals) when comparing the mean absolute error versus the experiment as presented in Table III. While we have not investigated the source of such deficiencies, we note that Bauschlicher and Partridge discovered that, on average, the 6–311 + G(3df,2p) basis set yields superior B3LYP atomization energies for this set of reactions than does the aug-cc-pVTZ basis set (from which our UCC basis is derived). They noted that the major difference between these two basis sets is the absence of a tight *d* function in the aug-cc-pVTZ basis (and thus, our UCC basis set as well). We did investigate this for the case of SO₂ (see below) but not otherwise. We would, however, expect that the tight *d* deficiency of the B3LYP/aug-cc-pVTZ results would be similarly reflected in our ACM/UCC results because uncontracting the primitives, while providing greater flexibility in the basis, would not make up for the absence of such functions and the ACM and B3LYP methods appear to behave quite similarly in general.

One final point regarding the quality of the UCC basis set concerns the calculated atomization energies of SO₂. Of the 54 G1 molecules considered in the present study, the SO₂ molecule stands alone with an anomalously large difference between the numeric results of Becke and our UCC results: for ACM the numeric method of Becke yielded 251.4 kcal/mol while our UCC result was 238.4 kcal/mol (13.0 kcal/mol difference); for BP91 the analogous values were 269.0 and 256.7 kcal/mol (12.3 kcal/mol difference). No other molecule of the G1 set exhibited differences (between the UCC atomization energies and the numeric results of Becke) even half as large as such differences for SO₂. To investigate this further, we performed single point ACM energy calculations (at the ACM/UCC optimized geometry) on SO₂ (plus O and S atoms) with larger correlation consistent basis sets designated herein as UCC4 and UCC5. We derived these basis sets by uncontract-

ing the *s*, *p*, *d* and *f* functions of the aug-cc-pVQZ and the aug-cc-pV5Z basis sets of Dunning et al.,⁵⁰ respectively. Furthermore, out of necessity, we deleted all basis functions with orbital angular momentum beyond *f*-type functions because, at present, our version of *Turbomole* cannot handle such functions. Our UCC4 basis set thus consisted of 13s7p4d3f for O and 17s12p4d3f for S and, similarly, our UCC5 basis set consisted of 15s9p5d4f for O and 21s13p5d4f for S. Furthermore, following the work of Bauschlicher and Partridge,²⁹ we investigated the effect of including tight *d* polarization functions (with exponents as prescribed in table 2 of ref. 29) on both sulfur and oxygen. The results of these calculations on SO₂ are summarized in Table IV.

As seen in Table IV, by expanding the UCC basis set to UCC4 we recovered 3.4 kcal/mol of the missing atomization energy. Similarly, we recovered an additional 4.5 kcal/mol in expanding the basis set from UCC4 to UCC5. The UCC5 atomization energy still remained 5.1 kcal/mol less than the exact result, however. As first noted by Bauschlicher and Partridge,²⁹ the tight *d* functions are important in describing this atomization reaction. Their effect is to increase the binding of SO₂ by 6.7, 4.6, and 1.2 kcal/mol for the UCC, UCC4, and UCC5 basis sets, respectively, with our best result (UCC5 + *d*) being 3.9 kcal/mol from the numeric basis set limit. This particular reaction, in contrast to commonly held belief, illustrates that in certain cases, DFT energies are very slowly convergent with respect to basis set.

TABLE IV. Comparison of ACM Atomization Energies of SO₂ (kcal / mol).

Basis Set	Atomization Energy
UCC	238.4
UCC4	241.8
UCC5	246.3
UCC + tight <i>d</i> ^a	245.1
UCC4 + tight <i>d</i> ^a	246.4
UCC5 + tight <i>d</i> ^a	247.5
Numeric ^b	251.4
Experiment ^c	254.0

^aRefer to ref. 29, table 2 for tight *d*-function orbital exponents.

^bRef. 18.

^cRef. 45.

We should also note that SO_2 was found to be a challenge for other accurate quantum methods in that the G1 and G2 total energies for SO_2 differed by an unusually large amount (8.8 kcal/mol)⁴⁶ attributed to the addition of a third d polarization function to the O and S basis sets in the G2 method, and the error in the G2 atomization energy of SO_2 was still unusually large (5.1 kcal/mol).⁴⁶

Focusing again on Table III, we can also use this data to compare the practical performance of Becke's original formulation of ACM to B3LYP for this set of atomization reactions. It appears that, on average, B3LYP may have some slight advantages. We suggest this for two reasons. First, in comparing the B3LYP/aug-cc-pVTZ and ACM/UCC (uncontracted aug-cc-pVTZ) results, we would expect, all else being equal, that the UCC basis set would perform better. Because, however, the opposite was found (i.e., the B3LYP/aug-cc-pVTZ mean absolute deviation was 0.5 kcal/mol smaller than that for ACM/UCC), this seems to indicate that all else was not equal and that B3LYP was slightly preferable. We note that the maximum deviation (that for SO_2) was 4.8 kcal/mol larger for B3LYP/aug-cc-pVTZ than for ACM/UCC. This is not surprising in that this particular reaction was very strongly dependent on the basis set (see above). Second, because both the aug-cc-pVTZ + d and the 6-311 + G(3 df , 2 p) B3LYP mean absolute deviations were slightly smaller than that for the fully numeric ACM coupled with the fact that the fully numeric ACM results were the best possible ACM results for this set of reactions, this again would suggest that B3LYP may have a slight practical advantage. We have not carried out a direct, comprehensive comparison of the overall practical performance of these two hybrid methods over a wide range of molecules/properties, so we stress that the conclusions drawn above are very limited in scope.

Finally, we should comment on the fact that the mean absolute theory versus the experiment errors for the set of 54 G1 atomization energies were significantly less than those when all 108 atomization reactions were considered (column 2 of Table II). For example, the ACM/UCC mean absolute error was 3.0 kcal/mol for the 54 molecule subset while it was 4.1 kcal/mol for the full set of 108 molecules. Likely causes for such behavior are that the experimental data and/or the theoretical results were more accurate for the G1 subset than for the other reactions. We feel it was probably a combination of the two effects because the

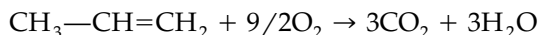
molecules of the G1 set were selected specifically because there was very reliable experimental data available; and the remaining 54 molecules were, in general, larger than the G1 molecules, and certain types of systematic errors due to deficiencies in the theory became proportionally larger with system size.

Considering next the hydrogenation reactions (Table II, column 4), ACM had the lowest mean error with any of the basis sets considered; again, the ACM/UCC method was the overall best result (mean error of 3.7 kcal/mol). This class of reactions is clearly distinct from the atomization and bond dissociation classes in that, with the 6-31G** basis set, MP2 performed, on average, identically to ACM. Furthermore, HF (which performed very poorly for atomization and bond dissociation reactions) actually performed better than all but ACM and MP2. Additionally, the VWN method did much better for the hydrogenation reactions than for the reactions considered above.

The performance for the oxygenation reactions is tabulated in column 5 of Table II. The most notable feature of this reaction class is the overall poor performance of all methods, and particularly, the NLDFT methods. This was the only reaction class considered for which no method achieved a mean accuracy of 10 kcal/mol or better. (In fact, for all the other reaction classes, at least one method performed better than 5 kcal/mol accuracy.) All of the DFT methods exhibited a strong basis set dependence (with a 10-15 kcal/mol improvement in accuracy in progressing from the DZP and 6-31G** basis sets to the UCC basis set), and there may well still be significant basis set errors even with the UCC basis set. There is little doubt, however, that all four of the density functionals are deficient in describing reactions of this type. Perhaps the most surprising observation is that, among the DFT methods, VWN performed consistently and significantly better than any of the NLDFT methods for every basis set considered.

Can we explain this anomalous behavior? First, we note that the same poor performance was observed by Nicolaides and Radom⁵⁶ with the G2 method.⁴⁶ In that study, Nicolaides and Radom attributed the failure of G2 in predicting heats of combustion to relatively large errors in the G2 energies of O_2 and CO_2 (2.4 and 2.7 kcal/mol error in the heats of atomization of O_2 and CO_2 , respectively) and the fact that the signs of the errors were such that they were additive when considering combustion processes. Thus, they found, for exam-

ple, that the G2 method when applied to the combustion reaction



was in error by 20.3 kcal/mol.

We found similar behavior for ACM/UCC for which the errors in atomization energies of O_2 , CO_2 , and H_2O were 3.3, 1.2, and 2.8 kcal/mol, respectively; and the signs of the errors were such that they were additive for combustion reactions. For the reaction above, ACM/UCC was in error by 25.7 kcal/mol. Based on such an analysis (i.e., analyzing the reaction energies as sums and differences of atomization energies), it appears that the anomalously large errors found for oxygenation reactions were an unfortunate consequence of error additivity. As listed above, none of the ACM/UCC errors associated with the atomization energies of O_2 , CO_2 , and H_2O were unusually large. (All were below the mean ACM/UCC error for atomization reactions, which is slightly greater than 4 kcal/mol.) However, for any reaction in which O_2 is a reactant and H_2O and CO_2 are products (or vice versa), the errors all contribute in the same direction (i.e., their effects are additive rather than cancelling); and for reactions such as the one above, the additive errors are amplified by the relatively large prefactors.

Interestingly, when we treated the above reaction with the VWN/UCC method (on average, the best of the DFT methods for the oxygenation reactions examined), we found a theory versus experiment difference of only 1.2 kcal/mol, an excellent agreement, particularly when compared to the NLDFT methods or the G2 method. However, if again we considered this combustion reaction by taking sums and differences of the atomization energies of the reactants and products, the excellent agreement between VWN/UCC and experiment was found to be the result of cancellation of large errors: the VWN/UCC energies of atomization for propene, O_2 , CO_2 , and H_2O were *in error* by 107.0, 53.3, 80.1, and 35.1 kcal/mol, respectively.

The MP2/6–31G** method performed best for this class of reactions (mean error of 11.2 kcal/mol). However, this result was most probably the result of cancellation of errors (as for VWN/UCC above) in that it is well known that the G2 method yields more accurate thermochemical data than does MP2. Nonetheless, without the use of some sort of empirical correction, such as that proposed by Nicolaides and Radom,⁵⁶ it appears that, among the

methods considered in the present study, MP2 is the best choice for studying combustion reaction energies.

The results for energies of isomerization reactions are listed in Table II, column 6. Note that for this reaction class (as well as the isodesmic reaction class, column 7 of Table II, see discussion below), only a relatively small number of suitable reactions could be constructed from our set of 108 molecules. Therefore, the data in these two columns should be regarded as substantially less complete than that for the other reaction classes. The 12 isomerization reactions represented by this data include relative energies of four isomers of CH_2N_2 (cyanoamine, HNCNH , diazomethane, and diazirine), three isomers of $\text{C}_2\text{H}_4\text{O}$ (acetaldehyde, vinyl alcohol, and ethylene oxide), three isomers of C_3H_4 (propyne, allene, and cyclopropene), $\text{HCN} \leftrightarrow \text{HNC}$, acetylene \leftrightarrow vinylidene, $\text{HNCO} \leftrightarrow \text{HCNO}$, 1,3,5-oxadiazole \leftrightarrow 1,2,4-oxadiazole, and *trans*-diimine \leftrightarrow *cis*-diimine. As a whole, all methods performed well for this reaction class with all but HF/6–31G** within 5.5 kcal/mol of the experiment and with the NLDFT mean errors falling in the range of 3.5–4.5 kcal/mol. One interesting feature of this reaction class was that the more complete basis set calculations, on average, performed less well than those using double- ζ type basis sets: for ACM the best basis set was DZP (3.6 kcal/mol), for BLYP it was 6–31G** (3.9 kcal/mol), for VWN it was also 6–31G** (5.1 kcal/mol), and for the one exception, BP91, the best basis set was TZ2P (3.6 kcal/mol). Of the 12 isomerization reactions considered, the one reaction that was, perhaps, most problematic for the DFT methods was the propyne \leftrightarrow allene isomerization. Experimentally, propyne was found to be slightly more stable (1.0 kcal/mol) than allene. However, as summarized in Table V, all of the DFT-based methods considered predicted allene to be slightly more stable than propyne.

Quantitatively, the DFT errors with respect to the experimentally determined value were not unusually large (3–6 kcal/mol), and the more complete basis sets tended to lower the relative energy of propyne. However, it does appear that the basis set limits of each of the density functionals predicted the incorrect order for these two isomers whereas HF and post-HF results consistently favor propyne.⁵⁷

Column 7 of Table II lists the performance of the methods for the eight isodesmic reactions considered. As noted above, because the number of reactions included in this class was relatively small,

TABLE V.
Calculated Heats of Reaction (kcal / mol) for Propyne → Allene Isomerization.

	HF	MP2	VWN	BLYP	BP91	ACM
DZP	—	—	−4.28	−3.93	−3.74	−2.58
6-31G**	1.28	4.35	−4.67	−4.40	−4.27	−3.08
DZVP	—	—	−4.10	−3.70	−3.65	−2.49
TZVP	—	—	−3.64	−3.36	−3.38	−2.25
TZ2P	—	—	−3.64	−3.37	−3.30	−2.19
UCC	—	—	−3.51	−3.24	−3.19	−2.12

any conclusions made must be considered preliminary. For these reactions, the HF/6-31G** method was best overall (2.5 kcal/mol mean absolute error), and the MP2/6-31G** (3.0 kcal/mol mean absolute error) also performed well. The ACM and BLYP functionals also performed well and show comparable behavior as a function of the basis set, with the mean absolute errors for the DZVP, TZVP, TZ2P, and UCC basis sets all falling in the range 2.9–3.4 kcal/mol. The performance of BP91 was similar to, but consistently less accurate than, ACM and BLYP for the isodesmic reactions. VWN was the least appropriate method for this reaction class with any of the basis sets. Overall, the data for this reaction class seem to suggest that it is better to neglect electron correlation entirely than to include it in an approximate way if one wants to take advantage of the unique behavior of cancellation of energy errors in isodesmic reactions.

The final reaction class (tabulated in the last column of Table II) contains a variety of reactions that do not fit into any of the reaction classes discussed above. This class includes fluorination reactions, chlorination reactions, addition of ammonia, addition of water, addition of methane, bond dissociation/creation reactions involving more than one bond, and other types of reactions. Rather surprising for such a mix of reactions, the HF method had the lowest mean error of any of the 6-31G** methods considered (4.3 kcal/mol). However, 6-31G** appeared to be a poor basis set choice for reactions in this category; and, as the basis set was improved, the accuracy of all of the DFT-based methods improved, with the most accurate method overall being ACM/UCC (2.2 kcal/mol).

MOLECULAR GEOMETRIES

In analogy to the reaction energy analysis above, we compared the performance of each of the theoretical methods using experimental structural

data⁵⁸ as our standard. The results of such a comparison are presented in Table VI as follows: column 2 includes data for all bond distances; column 3 for bond distances involving first row atoms (and H) only; column 4 for bond distances involving at least one second-row atom; column 5 for bond distances involving at least one hydrogen atom; column 6 for bond distances that do not involve a hydrogen atom; and column 7 for all bond angles.

In considering the geometrical data in Table VI as a whole, based on mean absolute errors, ACM was clearly superior for any type of geometrical parameter regardless of basis set choice. This finding was perhaps unexpected in that the ACM coefficients chosen by Becke¹⁸ were optimized for reproducing experimental atomization energies for the G1 set of molecules⁴⁵ (i.e., no consideration was given to molecular geometry). Of the remaining DFT methods, each had its relative strengths and weaknesses. The BP91 method was generally good for bond distances involving first-row elements but did not perform well for bond distances involving at least one second-row element. VWN did well for bond distances that did not involve hydrogen but performed poorly for bond distances that did. BLYP was generally not a good choice for bond distances as BLYP bond distances are usually significantly too long (see Table VII). For bond angles, VWN, BP91, and BLYP performed similarly with VWN better with DZ-quality basis sets but BP91 and BLYP better with the larger basis sets. Considering the MP2/6-31G** results, overall, MP2 geometries were superior to all but ACM with the exception of second-row distances and bond distances not involving hydrogen. Finally, the HF/6-31G** results were typically similar to or slightly worse than the pure DFT/6-31G** results with the exception of second-row bond distances for which HF performed better than all but ACM. This last observation was actually the result of the pure DFT methods (and MP2) per-

TABLE VI.**Mean Absolute Theory Vs. Experiment Errors of Symmetry–Unique Bond Distances (pm), Symmetry–Unique Bond Angles (Degrees), and Dipole Moments (Debye).**

Method	All r^a	First r^b	Second r^c	H r^d	no-H r^e	θ^f	μ^g
HF, 6–31G**	2.10	2.11	2.05	1.34	2.74	1.32	0.231
MP2, 6–31G**	1.46	1.30	2.45	0.88	1.95	1.10	0.205
VWN							
DZP	1.87	1.71	2.57	2.08	1.68	1.19	0.203
6–31G**	1.64	1.51	2.46	1.61	1.68	1.14	0.228
DZVP	1.64	1.48	2.63	1.61	1.67	0.97	0.190
TZVP	1.38	1.24	2.34	1.41	1.34	1.06	0.195
TZ2P	1.30	1.25	1.66	1.26	1.33	0.98	0.139
UCC	1.31	1.26	1.75	1.32	1.31	0.99	0.104
BLYP							
DZP	2.22	1.75	4.38	1.92	2.48	1.26	0.182
6–31G**	2.08	1.66	4.16	1.42	2.63	1.23	0.197
DZVP	2.42	2.05	4.40	1.42	3.27	0.98	0.148
TZVP	2.03	1.61	4.28	1.15	2.79	0.95	0.164
TZ2P	1.63	1.31	3.32	1.00	2.15	0.97	0.101
UCC	1.55	1.22	3.42	1.02	2.04	0.91	0.059
BP91							
DZP	1.90	1.48	3.74	1.80	1.99	1.25	0.162
6–31G**	1.68	1.33	3.30	1.32	1.97	1.20	0.188
DZVP	1.94	1.63	3.40	1.30	2.47	0.97	0.151
TZVP	1.59	1.25	3.33	1.13	1.99	0.92	0.147
TZ2P	1.30	1.05	2.52	1.00	1.56	0.98	0.092
UCC	1.22	0.96	2.51	1.03	1.58	0.92	0.067
ACM							
DZP	1.29	0.96	2.18	1.12	1.44	1.04	0.142
6–31G**	1.06	0.98	1.62	0.78	1.29	0.98	0.165
DZVP	1.11	1.13	1.70	0.82	1.36	0.87	0.194
TZVP	0.93	0.80	1.64	0.72	1.12	0.85	0.184
TZ2P	0.95	0.93	1.20	0.71	1.15	0.84	0.105
UCC	0.92	0.91	1.15	0.71	1.09	0.88	0.071

^aAll bond distances.^bBond distances involving first-row elements and H only.^cBond distances involving at least one second-row element.^dBond distances involving at least one H atom.^eBond distances involving no H atoms.^fAll bond angles.^gAll dipole moments.

forming unusually poorly rather than HF performing exceptionally well, in that the mean HF/6–31G** error was very similar for first-row and second-row bond distances (2.11 and 2.05 pm, respectively). Note that all of the DFT methods (particularly BP91 and BLYP) were significantly less accurate for bond distances involving second row elements.

The overall basis set dependence for molecular geometries was fairly consistent for all the DFT methods: as the basis set was improved the mean errors were reduced. There are two specific points worth noting, however. First, of the DZ-quality

basis sets, unlike the reaction energies where DZVP was superior, there was no clear preference for geometries: 6–31G** performed best for distances, but DZVP was best for angles. Second, we note that for geometrical parameters involving H and first-row elements only, the results were essentially converged with TZ-quality basis sets. However, for parameters involving second-row elements, there was often a significant change in going from the TZ-quality bases to the UCC basis.

Finally, we considered the signs of the theory versus experiment bond distance errors to assess whether there was a tendency for each of the

TABLE VII. **Number of Calculated Bond Distances that Overestimate Vs. Underestimate Distance Determined by Experiment.**

Method	All r ^a	First r ^b	Second r ^c	H r ^d	no-H r ^e
HF, 6–31G**	16 / 76	6 / 74	5 / 20	5 / 82	11 / 94
MP2, 6–31G**	100 / 89	55 / 24	22 / 4	23 / 61	77 / 28
VWN					
DZP	127 / 63	28 / 50	16 / 8	83 / 5	44 / 58
6–31G**	130 / 61	36 / 43	15 / 9	79 / 9	51 / 52
DZVP	137 / 54	45 / 34	15 / 9	77 / 11	60 / 43
TZVP	124 / 61	33 / 43	15 / 7	76 / 11	48 / 50
TZ2P	102 / 87	14 / 64	13 / 11	75 / 12	27 / 75
UCC	102 / 82	12 / 63	14 / 8	76 / 11	26 / 71
BLYP					
DZP	183 / 11	76 / 3	25 / 1	82 / 7	101 / 4
6–31G**	180 / 15	78 / 2	24 / 2	78 / 11	102 / 4
DZVP	181 / 14	79 / 1	24 / 2	78 / 11	103 / 3
TZVP	170 / 20	74 / 4	23 / 1	73 / 15	97 / 5
TZ2P	164 / 28	74 / 6	23 / 3	67 / 19	97 / 9
UCC	160 / 25	69 / 7	23 / 1	68 / 17	92 / 8
BP91					
DZP	167 / 24	60 / 16	25 / 1	82 / 7	85 / 17
6–31G**	173 / 21	70 / 9	25 / 1	78 / 11	95 / 10
DZVP	179 / 14	77 / 2	25 / 1	77 / 11	102 / 3
TZVP	160 / 26	65 / 13	23 / 1	72 / 12	88 / 14
TZ2P	150 / 37	56 / 19	24 / 2	70 / 16	80 / 21
UCC	146 / 37	53 / 20	22 / 2	71 / 15	75 / 22
ACM					
DZP	119 / 73	23 / 56	21 / 3	75 / 14	44 / 59
6–31G**	113 / 73	30 / 47	24 / 2	59 / 24	54 / 49
DZVP	123 / 68	46 / 34	24 / 2	53 / 32	70 / 36
TZVP	95 / 86	27 / 48	21 / 3	47 / 35	48 / 51
TZ2P	66 / 118	11 / 66	16 / 9	39 / 43	27 / 75
UCC	65 / 116	8 / 68	16 / 7	41 / 41	24 / 75

For each theoretical method an entry of the form $N_{>}/N_{<}$ appears in the table where $N_{>}$ is the number of calculated bond distances greater than experiment and $N_{<}$ is the number of calculated bond distances less than experiment.

^aAll bond distances.

^bBond distances involving first-row elements and H only.

^cBond distances involving at least one second-row element.

^dBond distances involving at least one H atom.

^eBond distances involving no H atoms.

methods to systematically overestimate or underestimate bond lengths. The relevant data are presented in Table VII where we have plotted $N_{>}/N_{<}$ for each level of theory (where $N_{>}$ is the number of distances greater than experimental measurement and $N_{<}$ is the number of distances less than experimental measurement).

Among the four DFT methods, BLYP and BP91 systematically overestimated bond distances for all bond classifications regardless of basis set choice. As indicated in Table VI, the magnitude of the overestimation was, on average, consistently larger for BLYP than for BP91. The behavior of the VWN

and ACM functionals depended on the bond type and the choice of basis set. For bonds involving at least one second-row atom and for bonds to hydrogen. VWN and ACM also showed a tendency to overestimate bond distances (although, for ACM, this tendency did not hold for bonds involving H with the three largest basis sets). The tendency for VWN to overestimate bonds involving hydrogen was quite strong and, in all cases, exceeded that of either BLYP or BP91. However, for bonds involving only first-row atoms and for bonds that do not include hydrogen, ACM and VWN were more or less neutral with the smaller basis sets and showed

a strong tendency to underestimate such distances with the two largest basis sets. Among the double- ζ basis sets, the DZVP basis set had the greatest tendency to overestimate bond distances of all types and, in fact, there was no DZVP data point for which $N_{<} \geq N_{>}$.

MOLECULAR DIPOLE MOMENTS

The last column of Table VI contains the results of our theory versus experiment comparison for molecular dipole moments. Again here, as above, we used experimental dipole moments⁵⁹ as our standard. Overall, it appeared that BLYP, BP91, and ACM were the most accurate methods for predicting dipole moments while VWN was consistently the least accurate of the functionals considered. For the four smallest basis sets (DZP, 6-31G**, DZVP, and TZVP), the mean errors ranged from 0.14 to 0.23 debye. There was no clear basis set preference among these four, although 6-31G** appeared to be the least appropriate. For these four basis sets, ACM performed best with the DZP and 6-31G** basis sets while BLYP and BP91 performed best with DZVP and TZVP.

It is well known that a good description of polarization and diffuse AOs are needed for accurate calculations of dipole moments, and the data in Table VI confirm this. Significant improvements in accuracy resulted in progressing from the first four basis sets (each of which includes only one set of polarization orbitals and no diffuse functions) to TZ2P (two polarization functions and no diffuse functions) and, again in progressing from TZ2P to UCC (additional p , d polarization functions, f polarization functions, and diffuse s , p , d , f functions). BLYP/UCC gave the lowest overall mean error (0.059 debye).

Conclusions and Recommendations

From the results presented above, we make the following conclusions and recommendations:

1. Based on the mean errors with respect to experimental data, ACM is the overall best choice for predictions of both reaction energies and geometries of first- and second-row molecular systems. For predictions of energies of reaction, we find the overall performance to be $\text{ACM} > \text{BP91} > \text{BLYP} \gg \text{VWN}$.

For predictions of molecular geometries, we find $\text{ACM} > \text{BP91}$, $\text{VWN} > \text{BLYP}$. ACM is also a good choice for predicting dipole moments, although BLYP and BP91 may be of comparable or better accuracy. However, note that for reaction energies, ACM generally performs best as one approaches basis set saturation. With moderate size basis sets, ACM may not be the best choice. In particular, for atomization and bond dissociation reactions, BP91 or BLYP with DZVP and TZVP basis sets are, on average, preferable.

2. Basis set choice is important. For high accuracy, large basis sets of at least TZ quality augmented with polarization functions are needed. For more routine use, the DZVP basis set appears to be the best choice currently available. Also, we caution that certain problems (e.g., the atomization energy of SO_2) require extremely large basis sets to be well treated.
3. NLDFT methodology offers much higher accuracy for prediction of heats of reaction than both HF and LDFT (at roughly the same computational cost). Additionally, the NLDFT methods are, in general, superior to MP2 for heats of reaction. However, there are examples where the BP91, BLYP, and ACM functionals perform poorly even with basis sets of near s , p , d , f saturation (e.g., the oxygenation reactions as a whole); thus, there is still a great need for functionals of higher accuracy.
4. Regarding computational cost, the NLDFT methods (particularly ACM, as stated in point 1) provide the best accuracy/cost ratio for calculation of chemical reaction energies and molecular dipole moments. For predictions of geometries, ACM provides the highest accuracy; however, VWN results may be satisfactory and require roughly half of the CPU time to evaluate the exchange-correlation potential than do the NLDFT methods. Furthermore, although we did not address this point in the present study, one can evaluate the Coulomb potential with approximate techniques^{6–9, 60} that will dramatically reduce the cost of any of the methods that do not require the traditional evaluation of two-electron integrals for the exchange energy (i.e., any of the “pure” DFT methods). For example, results from the recent work of Eichkorn

et al. (in which the Coulomb potential was obtained by approximating the density in terms of an atom-centered auxiliary basis set) indicate that the CPU cost reduction is in the range of 4–10X.⁶⁰ This raises the question of whether the accuracy gain from ACM (vs. BLYP and BP91) is worth the cost of explicitly calculating the two-electron integrals. At this point, we can only answer this question by stating that unless and until more accurate pure DFT methods are developed, there will certainly be problems where the added accuracy of ACM is necessary and thus the additional cost would be justified. Ongoing and future developments in techniques for evaluating the Coulomb and exchange potentials (e.g., the so-called order (N) fast multipole method⁴⁰) may obviate this question by eliminating the traditional, analytical evaluation of two-electron integrals entirely, regardless of functional choice.

5. Points 1–4 above are based on the performance of each of the methods on average. However, when choosing a method to use for a particular problem, one would like to know the best method to use “for that problem.” This is not the same as the best method “on average.” We, therefore, recommend that one refer to the raw data available as Supplementary Material⁵¹ to identify systems that are similar in bonding/electronic structure to the system of interest to help select the best method to use.

One final note: throughout our analysis, we made the underlying assumption that all of the experimental reference data were absolutely accurate. Certainly, this was a false assumption. We made efforts to select reliable experimental data,^{52,58,59} but most probably, some (a small number, we presume) of the experimental values used in our theory versus experiment analyses were inaccurate. We believe that this assumption has not caused any of the conclusions and recommendations stated above to be qualitatively incorrect. At worst, some of the mean absolute errors and their standard deviations would shift slightly were we able to identify and replace the incorrect experimental values with correct ones. In fact it is likely that, for the more accurate theoretical methods, the theory versus experiment errors would be further reduced.

Acknowledgments

This work was supported, in part, by a grant to Biosym Technologies from the National Institute of Standards and Technology/Advanced Technology Program. Preliminary reports of this work have appeared elsewhere.⁶¹

References

1. J. Labanowski and J. Andzelm, Eds., *Density Functional Methods in Chemistry*, Springer-Verlag, New York, 1991.
2. T. Ziegler, *Chem. Rev.* **91**, 651 (1991) and references therein.
3. J. Andzelm and E. Wimmer, *J. Chem. Phys.*, **96**, 1280 (1991).
4. B. G. Johnson, P. M. W. Gill, and J. A. Pople, *J. Chem. Phys.*, **98**, 5612 (1993).
5. N. C. Handy, D. J. Tozer, G. J. Laming, C. W. Murray, and R. D. Amos, *Israel J. Chem.*, **33**, 331 (1993).
6. *DMol, Version 9.5.0*, Biosym/Molecular Simulations Inc., San Diego, CA, 1995.
7. *DGauss*, Cray Research Inc., Eagan, MN.
8. *deMon*, Université de Montréal, Québec, Canada.
9. *ADF*, Vrije Universiteit, Amsterdam, The Netherlands; Biosym/Molecular Simulations, Inc., San Diego, CA, 1995.
10. (a) P. Hohenberg and W. Kohn, *Phys. Rev. B*, **136**, 864 (1964); (b) W. Kohn and L. J. Sham, *Phys. Rev. A*, **140**, 1133 (1965).
11. R. G. Parr and W. Yang, *Density Functional Theory of Atoms and Molecules*, Oxford University Press, New York, 1989, appendix A.
12. J. C. Slater, *Quantum Theory of Molecules and Solids*, vol. 4, McGraw-Hill, New York, 1974.
13. S. H. Vosko, L. Wilk, and M. Nusair, *Can. J. Phys.*, **58**, 1200 (1980).
14. D. M. Ceperley and B. J. Alder, *Phys. Rev. Lett.*, **48**, 566 (1980).
15. A. D. Becke, *Phys. Rev. A*, **38**, 3098 (1988).
16. C. Lee, W. Yang, and R. G. Parr, *Phys. Rev. B*, **37**, 785 (1988).
17. J. P. Perdew, In *Electronic Structure of Solids*, P. Ziesche and H. Eschrig, Eds., Akademie Verlag, Berlin, Germany, 1991.
18. A. D. Becke, *J. Chem. Phys.*, **98**, 5648 (1993).
19. V. Barone, *Chem. Phys. Lett.*, **226**, 392 (1994).
20. A. Ricca and C. W. Bauschlicher, *J. Phys. Chem.*, **98**, 12899 (1994).
21. Z. Latajka, Y. Bouteiller, and S. Scheiner, *Chem. Phys. Lett.*, **234**, 159 (1995).
22. J. W. Andzelm, D. T. Nguyen, R. Eggenberger, D. R. Salahub, and A. T. Hagler, *Comput. Chem.*, **19**, 145 (1995).
23. C. Adamo, V. Barone, and F. Fortunelli, *J. Chem. Phys.*, **102**, 384 (1995).
24. J. Baker, M. Muir, and J. Andzelm, *J. Chem. Phys.*, **102**, 2063 (1995).
25. J. Baker, J. Andzelm, M. Muir, and P. R. Taylor, *Chem. Phys. Lett.*, **237**, 53 (1995).
26. J. E. Del Bene, W. B. Person, and K. Szczepaniak, *J. Phys. Chem.*, **99**, 10705 (1995).

27. M. Holthausen, C. Heinemann, H. H. Cornehl, W. Koch, and H. Schwarz, *J. Chem. Phys.*, **102**, 4931 (1995).
28. T. V. Russo, R. L. Martin, and P. J. Hay, *J. Chem. Phys.*, **102**, 8023 (1995).
29. C. W. Bauschlicher and H. Partridge, *Chem. Phys. Lett.*, **240**, 533 (1995).
30. C. W. Bauschlicher, *Chem. Phys. Lett.*, **246**, 40 (1995).
31. J. Baker, M. Muir, J. Andzelm, and A. Scheiner, In *Chemical Applications of Density-Functional Theory*, B. B. Laird, R. B. Ross, and T. Ziegler, Eds., American Chemical Society, Washington, D.C., 1996.
32. (a) C. W. Bauschlicher and H. Partridge, *J. Chem. Phys.*, **103**, 1788 (1995); (b) C. W. Bauschlicher and H. Partridge, *Chem. Phys. Lett.*, **245**, 158 (1995).
33. A. M. Mebel, K. Morokuma, and M. C. Lin, *J. Chem. Phys.*, **103**, 7414 (1995).
34. *Turbomole, Version 9.5.0*, Biosym/Molecular Simulations, Inc., San Diego, CA, 1995.
35. R. Ahlrichs, M. Bär, M. Ehrig, M. Häser, H. Horn, and C. Kölmel, *Chem. Phys. Lett.*, **162**, 165 (1989).
36. V. I. Lebedev, *Zh. Vychisl. Mater. Fiz.*, **15**, 48 (1975); V. I. Lebedev, *Zh. Vychisl. Mater. Fiz.*, **16**, 293 (1976).
37. A. D. Becke, *J. Chem. Phys.*, **88**, 2547 (1988).
38. B. Delley, In *Modern Density Functional Theory: A Tool for Chemistry*, P. Politzer and J. M. Seminario, Eds., Elsevier, New York, 1995.
39. O. Treutler and R. Ahlrichs, *J. Chem. Phys.*, **102**, 346 (1995).
40. B. G. Johnson, In *Modern Density Functional Theory: A Tool for Chemistry*, P. Politzer and J. M. Seminario, Eds., Elsevier, New York, 1995.
41. C. W. Murray, G. J. Laming, N. C. Handy, and R. D. Amos, *Chem. Phys. Lett.*, **199**, 229 (1992).
42. C. van Wüllen, *Chem. Phys. Lett.*, **219**, 8 (1994).
43. B. Delley, *J. Chem. Phys.*, **94**, 7245 (1991).
44. J. Baker, J. Andzelm, A. Scheiner, and B. Delley, *J. Chem. Phys.*, **101**, 8894 (1994).
45. (a) J. A. Pople, M. Head–Gordon, D. J. Fox, K. Raghavachari, and L. A. Curtiss, *J. Chem. Phys.*, **90**, 5622 (1989); (b) L. A. Curtiss, C. Jones, G. W. Trucks, K. Raghavachari, and J. A. Pople, *J. Chem. Phys.*, **93**, 2537 (1990).
46. L. A. Curtiss, K. Raghavachari, G. W. Trucks, and J. A. Pople, *J. Chem. Phys.*, **94**, 7221 (1991).
47. A. Schäfer, H. Horn, and R. Ahlrichs, *J. Chem. Phys.*, **97**, 2571 (1992).
48. P. C. Hariharan and J. A. Pople, *Theor. Chim. Acta (Berl.)*, **28**, 213 (1973).
49. N. Godbout, D. R. Salahub, J. Andzelm, and E. Wimmer, *Can. J. Chem.*, **70**, 560 (1992).
50. (a) T. H. Dunning, *J. Chem. Phys.*, **90**, 1007 (1989); (b) R. A. Kendall, T. H. Dunning, and R. J. Harrison, *J. Chem. Phys.*, **96**, 6796 (1992); (c) D. E. Woon and T. H. Dunning, *J. Chem. Phys.*, **98**, 1358 (1993).
51. Complete tables of molecular energies, geometries, and dipole moments as well as energies of reaction for all reactions considered in the present study may be obtained as Supplementary Material from the *Journal of Computational Chemistry*.
52. S. G. Lias, J. E. Bartmess, J. F. Liebman, J. L. Holmes, R. D. Levin, and W. G. Mallard, *J. Phys. Chem. Ref. Data*, **17** (Suppl. 1) (1988).
53. (a) A. D. Becke, *J. Chem. Phys.*, **88**, 2547 (1988); (b) A. D. Becke and R. M. Dickson, *J. Chem. Phys.*, **89**, 2993 (1988); (c) A. D. Becke and R. M. Dickson, *J. Chem. Phys.*, **92**, 3610 (1990); (d) A. D. Becke, *Int. J. Quantum Chem. Symp.*, **23**, 599 (1989).
54. P. J. Stevens, F. J. Devlin, C. F. Chabalowski, and M. J. Frisch, *J. Phys. Chem.*, **98**, 11623 (1994).
55. A. D. Becke, *J. Chem. Phys.*, **97**, 9173 (1992).
56. A. Nicolaides and L. Radom, *J. Phys. Chem.*, **98**, 3092 (1994).
57. W. J. Hehre, L. Radom, P. v. R. Schleyer, and J. A. Pople, *Ab Initio Molecular Orbital Theory*, Wiley-Interscience, New York, 1986.
58. (a) D. R. Lide, Ed., *Handbook of Chemistry and Physics*, 74th ed., CRC Press, Boca Raton, FL, 1993; (b) L. E. Sutton, Ed., *Tables of Interatomic Distances and Configuration in Molecules and Ions*, The Chemical Society Special Publications 11 and 18, The Chemical Society, London, 1958, 1965; (c) K.-H. Hellwege, Ed., *Landolt–Börnstein: Numerical Data and Functional Relationships in Science and Technology: Structure Data of Free Polyatomic Molecules*, new series II/7, Springer-Verlag, New York, 1976; (d) K. P. Huber and G. Herzberg, *Molecular Spectra and Molecular Structure IV. Constants of Diatomic Molecules*, Van Nostrand Reinhold Co., London, 1979; (e) B. Starck et al., *Bibliography of Microwave Spectroscopy, 1945–1975*, Eggenstein-Leopoldshafen: Zentralstelle für Atomkernenergie-Dokumentation, 1977; (f) B. J. Smith and L. Radom, *J. Am. Chem. Soc.*, **112**, 7525 (1990); (g) L. Halonen and T. K. Ha, *J. Chem. Phys.*, **89**, 4885 (1988); (h) J. Koput, *J. Mol. Spectrosc.*, **115**, 438 (1986); (i) C. Yamada and E. Hirota, *Phys. Rev. Lett.*, **56**, 923 (1986).
59. (a) *Landolt–Börnstein: Numerical Data and Functional Relationships in Science and Technology: Molecular Constants*, vols. 4, 6, 14, 19, Springer-Verlag, New York, 1967, 1974, 1982, 1992; (b) R. D. Nelson, D. R. Lide, and A. A. Maryott, *Selected Values of Electric Dipole Moments in the Gas Phase*, U.S. Government Printing Office, Washington, D.C., 1967; (c) A. L. McClellan, *Tables of Experimental Dipole Moments*, Freeman, San Francisco, 1963; (d) H. Kanata, S. Yamamoto, and S. Saito, *J. Mol. Spectrosc.*, **131**, 89 (1988).
60. K. Eichkorn, O. Treutler, H. Öhm, M. Häser, and R. Ahlrichs, *Chem. Phys. Lett.*, **242**, 652 (1995).
61. (a) 34th Sanibel Symposium, St. Augustine, FL, 1994; (b) 209th American Chemical Society National Meeting, Anaheim, CA, 1995; (c) 6th International Conference on the Applications of the Density Functional Theory in Chemistry and Phys., Paris, France, 1995; (d) J. Andzelm, J. Baker, A. Scheiner, and M. Wrinn, *Int. J. Quantum Chem.*, **56**, 733 (1995).